Response to Report 1

Referee Comment: *The paper does not mention any possible candidate materials where this effect can be realized. Especially, the condition that there are only two-nodes with c rage greater than one with finite tilt makes the model very restrictive.*

Our Response : We thank the referee for raising this point. In this work, we have investigated the Kerr and Faraday rotations for time-reversal symmetry (TRS) broken type-I (i.e., tilt parameter $|C_s| < 1$) multi-Weyl semimetals (mWSMs) containing a pair of Weyl nodes with opposite chiralities. In the case of a TRS broken mWSM containing more than one pair of nodes, the conductivity can be obtained by considering linear superposition of the results for individual pairs, which, as a result, would only modify the Kerr and Faraday rotations quantitatively.

We would like to point out that the TRS broken type-I single WSM phase ($n = 1$) has recently been experimentally realized in $Co_3Sn_2S_2$ [Refs. Science **365**, 1278 (2019), Science **365**, 1282 (2019)] whereas the compound $HgCr_2Se_4$ (Refs. 7 and 18 in the revised manuscript) is proposed to be a TRS broken double-WSM ($n = 2$) candidate. Moreover, it has also been predicted that the cubic Dirac semimetal $A(MoX)_3$ (with A = Rb, TI; X = Te) can accommodate triple Weyl points ($n = 3$) by breaking its TRS (Ref. 21 in the revised manuscript). These materials can be the possible candidates to verify our results on Kerr and Faraday rotations presented in the current work. However, the TRS broken type-II mWSMs (i.e., $|C_s| > 1$) should also give rise to Kerr and Faraday rotations which is not the focus of this work and we leave it for future study. We have now added a relevant comment on the possible candidate materials with appropriate references in the conclusion section of the revised manuscript (First paragraph, Left column, Page 11).

Referee Comment: *The paper doesn't provide any analysis of energy scales. This is important because of many factors, especially the fact that continuum model is applicable only in a very tiny energy and momentum window for most Weyl semi-metals. Usually, there are many electronic bands in the vicinity of Weyl node and it's difficult to disentangle the contributions arising from trivial bands and topological band crossings. For most materials even a two-band tightbinding model fails to capture these essential features as even the matrix elements between topological trivial bands start to contribute to conductivity. It would be helpful if authors can provide some estimate of energy and momentum cutoffs they have used in the continuum model on the basis of electronic band structure of existing topological weyl semimemetals.*

Our Response : We thank the referee for this comment. We agree with the referee that the continuum model is applicable in a small energy and momentum window, as it does not have the natural ultraviolet energy cutoff compared to the tight-binding model. At low frequencies, the lattice model of mWSMs is approximated by their corresponding low energy model, thus the optical conductivity obtained from the lattice and continuum models are in good agreement (Refs. 36 and 42 in the revised manuscript). On the other hand, as the frequency increases, optical conductivity deviates from the continuum model. Therefore, to make the continuum model work properly, one need to introduce the momentum cutoff as well as frequency cutoff. We have chosen the momentum cutoff along the k_z direction $k_c \sim \pi/a$ with $k_c > Q$ and consequently, $\omega_c = vk_c$. In particular,

we have taken $\hbar\omega_c/\mu = 70$ throughout the work. We have now added a relevant comment on this in the revised manuscript (First Paragraph, Right Column, Page 4).

In this work, the other parameters are chosen based on a typical Weyl semimetal. For example, we have chosen : $v = 10^6$ m/s, $Q = 5 \times 10^8$ m^{-1}, $\mu = 0.1$ eV and tilt velocity $= 0.4v$ for type-I case.

Referee Comment: *I don't understand how can one measure Faraday rotation in semi-infinite geometry. Could authors please clarify what is meant by Faraday angle in Eq. 28. The Kerr rotation can be measured directly from the quantities evaluated in Eq. 27 but Faraday rotation also depends on the path light traverses inside the material. Here, it's not so clear how would one measure the effect on the other end of the sample in semi-infinite geometry. Maybe, one can consider a bulk sample but given that the system here exhibit circular dichroism and circular birfringence so the rotation would also depend on the length of the sample. If I'm not missing something important here, this issue seems very concerning.*

Our Response : We thank the referee for raising this important point. In this work, we theoretically investigate the polarization rotation of reflected (Kerr rotation) and transmitted (Faraday rotation) light for two cases: (i) thin-film geometry and (ii) semi-infinite geometry. In the case of semi-infinite geometry, we consider only one interface (air-mWSM interface). Applying the proper boundary conditions for electric and magnetic fields at the interface, we obtain the transmission coefficients ($t_-, t_+, t_\parallel$ and $t_\perp$) for the transmitted light refracted from the interface and propagating through mWSM. Therefore, as pointed out by the referee, from an experimental standpoint, one cannot measure the obtained quantity χ_F^F, χ_F^V (which are calculated using $t_-, t_+, t_\parallel$ and $t_\perp$) and its related polarization rotations proposed in this work in experiment due to semi-infinite geometry.

However, despite using semi-infinite geometry in the current work, one can measure the polarization rotation for the transmitted light based on our results by considering a bulk mWSM of thickness d (as again pointed out by the referee) as explained below.

In this work, we analytically show that, for Faraday geometry, after incident on the mWSM interface, a linearly polarized light is divided into two circularly polarized eigenmodes (left and right circular) and propagate through the mWSM with different amplitudes and velocities. This fact leads to circular dichroism (CD) and circular birefringence (CB), which results from different absorptions and different speeds of two opposite circularly polarized light and are determined by the $\mathrm{Im}[\mathrm{n}_+ - \mathrm{n}_-]$ and $\mathrm{Re}[\mathrm{n}_+ - \mathrm{n}_-]$ respectively. Here, n_+, n_- are the index of refraction for left and right circularly polarized eigenmodes, respectively. It is well known that the polarization rotation of the transmitted light (i.e., Faraday rotation) and corresponding ellipcity are directly related to CB and CD, respectively. Therefore, using the Eq. (25) in the revised manuscript, one can measure the complex Faraday rotation for a bulk mWSM of thickness d as (Refs. Phys. Rev. B **96**, 195210 (2017), Small Methods **6**, 2200885 (2022))

$$\phi_{\mathrm{F}}^{\mathrm{Far}} = \Phi_{\mathrm{F}}^{\mathrm{Far}} + i\,\Psi_{\mathrm{F}}^{\mathrm{Far}}; \quad \Phi_{\mathrm{F}}^{\mathrm{Far}} = \frac{\pi d}{\lambda}\mathrm{Re}[\Delta \mathrm{n}] \quad \Psi_{\mathrm{F}}^{\mathrm{Far}} = \frac{\pi \mathrm{d}}{\lambda}\mathrm{Im}[\Delta \mathrm{n}] \tag{1}$$

where $\Delta n = n_+ - n_-$. Therefore, it is clear that the Faraday rotation ($\Phi_{\mathrm{F}}^{\mathrm{Far}}$) and corresponding ellipticity ($\Psi_{\mathrm{F}}^{\mathrm{Far}}$) are proportional to d in bulk mWSM. Since Δn is proportional to the topological charge, the Faraday rotation and corresponding ellipticity is also increases linearly with n. In the revised manuscript, similar analysis is also applied for

Voigt geometry case, where both linear birefringence and linear dichroism lead to a polarization rotation (Voigt rotation) of the transmitted light followed by the relation [Phys. Rev. Lett. **87**, 047401 (2001), Phys. Rev. B **89**, 085203 (2014)]: $\phi_{\rm F}^{\rm Voi} \approx \frac{\pi d}{i\lambda}(\mathrm{n}_{\parallel} - \mathrm{n}_{\perp})$. In the revised manuscript, we have now replaced the figures 4(c)-(d) and 5(c)-(d) by the new figures (Re[Δn] and Im[Δn]) and added a relevant comment on this with appropriate references (Second paragraph, Left column, Page 9; Third paragraph, Left column, Page 10), as well as modified abstract and conclusions.

Referee Comment: *Now, even, in the thin-film limit, the film thickness would play some role in deciding the Faraday rotation angle. The authors haved cited Ref. 51 which studies only Kerr and Faraday effect for monolayer graphene and hence the thickness of the sample doesn't come into picture. It would be very helpful if authors can make some comments about the range of thickness and compare it to the wavelength of the light used which in turn would depend on the energy scales of the system which are not discussed here. Also, would Kerr rotation be modified in any way, if we also consider the reflection at the other end of the sample.*

Our Response : We thank the referee for raising this question. In the thin-film limit ($d << \lambda$), the reflection and transmission coefficients $(r/t)_{ss,sp,ps,pp}$ which are used to calculate the Kerr and Faraday rotations are obtained from the surface conductivity σ_{ij}^{d} ($\sigma_{ij}^{d} = d\,\sigma_{ij}$) as can be seen from the Eq. (20) of the main text. In the case of Kerr rotation, it has been shown that the complex dimensionless quantity $\chi_{\rm K}^{p/s}$ for normal incidence is nearly independent of d and is mainly determined by the ratio $\sigma_{xy}^{d}/\sigma_{xx}^{d}$ (Refs. 41 and 42 in the revised manuscript). However, in the case of Faraday rotation, the complex dimensionless quantity $\chi_{\rm F}^{p/s}$ for normal incidence can be written as

$$\chi_{\rm F}^{p/s} = \frac{\sigma_{xy}^{d}}{\sigma_{1}^{d}} \propto \frac{d\,\sigma_{xy}}{(1+\frac{d\sigma_{xx}}{2c\epsilon_0})} \sim d\,\sigma_{xy} \quad d << \lambda. \tag{2}$$

It is clear from the above expression that the Faraday rotation is also proportional to d in the thin film limit. The thickness dependence of Kerr and Faraday rotations is depicted in Fig. 1.

In the thin-film limit, one has to satisfy the following criteria $a \ll d \ll \lambda$ (where a is the lattice constant and λ is the wavelength of the incident light). In the current work, we consider $d = 10-50$ nm and the wavelength of light λ is varied till near infrared wavelength range which satisfies the above criteria. For example, we have chosen Ω $(= \hbar\omega/\mu) = 5$ such that $\hbar\omega = 1$ eV and $\lambda \sim 1200$ nm, satisfying the condition $a \ll d \ll \lambda$. Furthermore, the energy cutoff in this low energy model is around 7 eV which is way above the incident photon energy.

Given the finite thickness (d) of the film, the two boundaries can act as a Fabry-Perot cavity, where scattering from both the interfaces can lead to an interference effect, which in turn can modify Kerr rotation. The maxima and minima conditions for this interference effect are $d = l\lambda/2$ and $d = (2l+1)\lambda/4$, where l is an integer. However, for thin-film limit ($\lambda \gg d$), which we are considering in the current work, the phase difference is negligible, resulting in minimal impact on the Kerr rotation. We have now added a relevant comment on this in the revised manuscript (First Paragraph, Left Column, Page 7).

Referee Comment: *I would like to reemphasize that authors should also provide some*

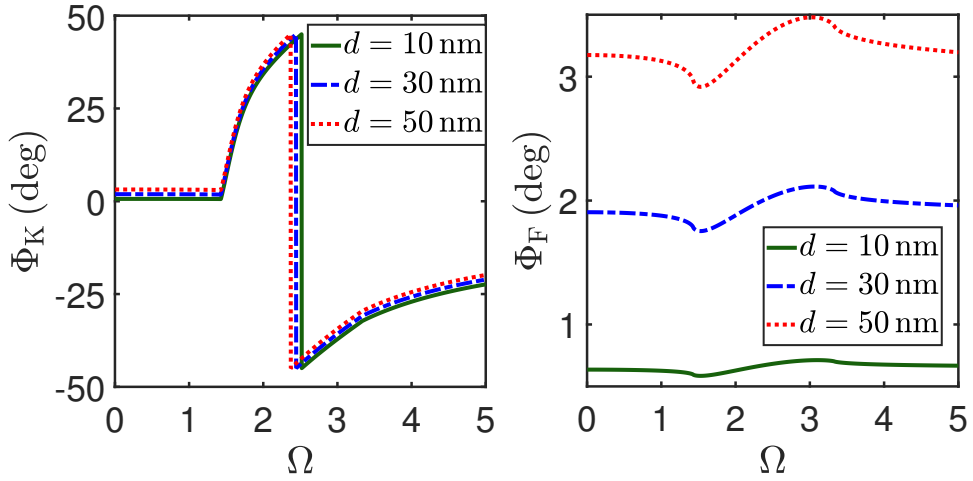

Figure 1: (a) Kerr angle and (b) Faraday angle as a function of thickness d for thin film limit of mWSMs. The rest of the parameters are the same as in Fig. 3 of the main manuscript.

estimate about the tilt as it decides the frequency range over which some of the quantities show a significantly important behavior. There is a minor typo in the paragraph below Eq. 9. The frequency range for the region in which the vertical transitions are Pauli unblocked should be $\omega > \omega_2$.

Our Response : We thank the referee for this comment. In mWSM, the range of the two photon energy bounds are dictated by the tilt parameter (C) of the Weyl node: $\hbar\omega_{1,2} = 2\mu/(1 \pm |C|)$. Since in the current work, we have restricted ourselves to a TRS broken tilted type-I mWSM, the range of C can be varied $0 < |C| < 1$ (tilt velocity $v_t = c\,v$). In the limit $C \to 0$ (small tilted type-I Weyl nodes), we have $\hbar\omega_1 \to \hbar\omega_2 \to 2\mu$. Therefore, the range of Pauli blocked region broadens and the region II disappears ($\omega_1 < \omega < \omega_2$). In this case, the real part of diagonal conductivity $\mathrm{Re}[\sigma_{ii}(\omega)]$ becomes finite for $\hbar\omega > 2\mu$ only. The imaginary part of the transverse conductivity vanishes whereas its real part have the intrinsic contribution (leading order is tilt independent) leading to Kerr rotation in thin film mWSM only in the region $\hbar\omega > 2\mu$. On the other hand, when $C \to 1$ (highly tilted type-I Weyl nodes), we have $\hbar\omega_1 \to \mu$ and $\hbar\omega_2 \to \infty$ leading to the fact that the region II ($\omega_1 < \omega < \omega_2$) will extend to very high energy. We have added a comment on this in the revised manuscript (First paragraph, Left column, Page 4). In addition, we have corrected the typo in the revised manuscript.

Referee Comment: *It would help if authors can provide the derivation for equation 16 and 17. It's not so clear how they divide the real part of the off-diagonal conductivity into DC and AC part. It seems that equation 16 is non-zero even in the DC limit. Another worrisome aspect of these equations (16-19) is that they diverge for zero tilt ($C = 0$). Could authors please provide an interpretation for $C = 0$ limit of these equations.*

Our Response: We thank the referee for this important question. We have now elaborated this part in the revised manuscript (Right Column, Page 5). The Eq. (16) in the main text, which is the real part of the off-diagonal conductivity $\sigma_{xy}(\omega)$, is derived from the imaginary part of $\sigma_{xy}(\omega)$ [Eq. (15) in the main text] using the Kramers-Kronig

relation. The real part of σ_{xy} can be written as

$$\begin{aligned}
\mathrm{Re}[\sigma_{xy}(\omega)] &= \frac{2}{\pi} P \int_0^{\omega_c} \frac{\omega' \mathrm{Im}[\sigma_{xy}(\omega')] d\omega'}{(\omega'^2 - \omega^2)} \\
&= \frac{6\,\mathrm{sgn}(C)}{\pi} \int_{\omega_1}^{\omega_2} \frac{\omega'\, \sigma^n_{\omega'}\, \kappa_0\, d\omega'}{(\omega'^2 - \omega^2)} = \mathrm{sgn}(C) \frac{e^2 n}{2\pi^2 \hbar v} \int_{\omega_1}^{\omega_2} \frac{\omega'^2\, \kappa_0\, d\omega'}{\omega'^2 - \omega^2}, \\
&= \mathrm{sgn}(C) \sigma^n_\mu \left[\frac{1}{|C|} - \frac{1}{2|C|^2} \ln \left| \frac{(\omega_2^2 - \omega^2)}{(\omega_1^2 - \omega^2)} \right| + \right. \\
&\left. \left(\frac{\mu}{2\hbar\omega |C|^2} + \frac{\hbar\omega}{8\mu |C|^2} - \frac{\hbar\omega}{8\mu} \right) \ln \left| \frac{(\omega_2 - \omega)(\omega_1 + \omega)}{(\omega_2 + \omega)(\omega_1 - \omega)} \right| \right]. \qquad (3)
\end{aligned}$$

It is important to note that $\sigma^{\mathrm{dc}}_{xy}(\omega = 0)$ (since the dc part is always real) has two contributions: i) intrinsic or 'universal' contribution $\sigma^{(\mathrm{in})}_{xy}$ and ii) free carrier contribution $\sigma^{(\mathrm{free})}_{xy}$. The $\sigma^{(\mathrm{free})}_{xy}$ can be extracted by taking the $\omega \to 0$ limit of the above equation. On the other hand, the intrinsic part, arising from the separation between the Weyl nodes, can be written as $\frac{e^2 n Q}{\pi h}$ (PRL **113**, 187202 (2014)). Therefore, the total dc contribution of σ_{xy} is given by

$$\begin{aligned}
\sigma^{\mathrm{dc}}_{xy}(\omega = 0) &= \frac{e^2 \mu n}{h^2 v} \left[\frac{2}{C} + \frac{1}{C^2} \ln \left(\frac{1 - C}{1 + C} \right) \right] + \frac{e^2 n Q}{\pi h} \\
&= \sigma^{(\mathrm{free})}_{xy} + \sigma^{(\mathrm{in})}_{xy}. \qquad (4)
\end{aligned}$$

However, one can obtain total dc contribution of σ_{xy} by substituting $\omega = 0$ in Eq. (3) of the main text, which can be written as

$$\begin{aligned}
&\mathrm{Re}[\sigma^{DC}_{xy}(\omega = 0)] \\
&= \frac{1}{(2\pi)^3} \sum_{s=\pm 1} s \int dk^3 \frac{f^{eq}_k}{2\hbar\omega_k} \left(\mathrm{Re}[(P^{-+})_x] \mathrm{Im}[(P^{-+})_y] - \mathrm{Im}[(P^{-+})_x] \mathrm{Re}[(P^{-+})_y] \right) \frac{2}{\omega_k} \\
&= \sigma^{(\mathrm{free})}_{xy} + \sigma^{(\mathrm{in})}_{xy}. \qquad (5)
\end{aligned}$$

In the case of an untilted mWSM (i.e., $C = 0$), the imaginary part of σ_{xy} vanishes, as the integrand involved in the calculation of σ_{xy} [Eq. (14) of the main text], reduced to an odd function. Consequently, the real part of $\sigma_{xy}(\omega)$, which was derived using the Kramers-Kronig relation in Eq. (16) (of the main text), vanishes for an untitled mWSM. However, the universal part of the off-diagoanl conductivity σ^{in}_{xy}, arising from the node separation Q, remains in the untilted mWSMs.